Microvascular Adaptation in the Cerebral Cortex of Adult Spontaneously Hypertensive Rats

SCOT L. HARPER, PH.D., AND H. GLENN BOHLEN, PH.D.

SUMMARY The purpose of this study was to determine the microvascular characteristics that cause cerebral cortical blood flow autoregulation to shift to a higher range of arterial pressures during established hypertension in spontaneously hypertensive rats (SHR). An open-skull technique with constant suffusion of artificial cerebrospinal fluid (PO_2 = 40–45 mm Hg, pCO_2 = 40–45 mm Hg, pH = 7.35–7.45) was used to view the parietal cortex of 18- to 21-week-old SHR and Wistar Kyoto (WKY) normotensive control rats. The resting inner diameters of first (1A)-, second (2A)-, and fourth (4a)-order arterioles were significantly ($p < 0.05$) smaller, and the wall thickness/lumen diameter ratios were significantly ($p < 0.05$) larger in SHR compared to WKY. Only 1A and 4A had significantly ($p < 0.05$) increased vessel wall cross-sectional area in SHR. At the resting mean arterial pressures of WKY and SHR, the passive (10^{-4} M adenosine, topical) diameters of comparable types of arterioles were not significantly different ($p > 0.05$). At reduced arterial pressures, however, the arterioles in SHR had smaller maximum diameters than in WKY. Cortical blood flow in WKY and SHR was constant at arterial pressures from 70–150 mm Hg and 100–200 mm Hg, respectively. Resting arteriolar pressures in 1A, 2A, and 3A of SHR were substantially and significantly ($p < 0.05$) elevated, although pressures in the smallest arterioles and venules of WKY and SHR were similar. Therefore, it is possible that cerebral capillary pressure is only slightly elevated, if at all, in SHR as a result of the vasoconstriction. The number of arterioles per unit area of brain surface at rest was equal in WKY and SHR. In addition, the number of vessels was equal in WKY and SHR during maximal dilation, and neither type of rat demonstrated an opening of previously closed vessels upon maximum dilation. Therefore, the cerebral arteriolar constriction in SHR, which was probably potentiated by vessel wall hypertrophy of the largest and smallest arterioles, was the major contributor to an upward shift in the autoregulatory range, the protection of exchange vasculature pressures, and the increase in vascular resistance. (Hypertension 6: 408–419, 1984)

KEY WORDS • microcirculation • hypertension • brain

ADAPTATION of the spontaneously hypertensive rat (SHR) to increased systemic arterial pressure must necessarily include mechanisms to protect the exchange vasculature from elevated microvascular pressures and potential overperfusion. This is especially important in the brain, where overperfusion can lead to edema and encephalopathy.[1-2] Some form of protection does exist in the SHR, since it is well established that cerebral blood flow (CBF) is maintained at normal or near normal levels in SHR and vascular resistance is increased.[3-5] Evidence is available to support an upward shift in the CBF autoregulatory range at the lower arterial pressure limits in hypertensive humans,[6, 7] baboon,[8] and SHR, [3, 9] and the upper arterial pressure limit in hypertensive baboons.[8] The increased cerebral vascular resistance and shift in the autoregulatory range during hypertension may be affected by generalized large and small vessel constriction, diminished capacity for maximum vasodilation,[8] and increased wall/lumen ratio accompanied by vascular wall hypertrophy.[10] There may also be an overall decrease in the density of perfused vessels, either on a temporary or permanent basis, as occurs in skeletal muscle of the SHR.[11-16]

We investigated the possibility that cerebral microvascular pressures near capillaries are normal in adult SHR as a result of increased resistance both of the large vessels upstream from the microcirculation and vessels comprising the microvasculature. It has been demonstrated by Kontos et al.[17] and Stromberg and Fox[18] in cats, and by our laboratory[19] in normal Wistar rats, that large arterial vessels preceding the microvasculature provide a substantial portion of both the arterial pressure dissipation and autoregulatory flow control. It is

From the Department of Physiology and Biophysics, Indiana University School of Medicine, Indianapolis, Indiana.

Supported by NIH Grant HL-20605. Dr. Bohlen is the recipient of a NIH Research Career Development Award, HL-01089.

Address for reprints: H. Glenn Bohlen, Ph.D., Department of Physiology and Biophysics, Indiana University School of Medicine, 635 Barnhill Drive, Indianapolis, Indiana 46223.

Received July 1, 1983; revision accepted November 22, 1983.

therefore reasonable to suspect that this large vessel control could also be adapted to the hypertensive state. If, as hemodynamic and anatomic[10] studies indicate, vascular hypertrophy is indeed present in cerebral vessels, it would be of interest to study whether this hypertrophy resulted in significant mechanical constriction and accentuated pressure dissipation across specific sections of the vasculature. In addition, it is conceivable that the lower end of autoregulation shifts to higher arterial pressures as a result of diminished capacity for dilation secondary to hypertrophy, and the upper end shifts because this same hypertrophy offers a mechanical advantage for supranormal constriction against the increase in transmural pressure. Either permanent or temporary vessel closure, or a combination thereof, may also simultaneously contribute to the increase in vascular resistance and subsequent shift in autoregulatory capabilities caused by vasoconstriction. Consequently, the number of perfused microvessels per unit surface area of brain was counted at rest and maximal vessel dilation to determine the relative roles of vascular caliber and density in the cerebral vascular adaptation to hypertension in SHR.

Methods

We studied 21 18- to 21-week-old spontaneously hypertensive rats (SHR) weighing 319 ± 41 (SD) g, and 19 age-matched Wistar-Kyoto controls weighing 352 ± 37 (SD) g. Animals were anesthetized with a saline solution of Inactin (Byk Gulden Konstanz, West Germany; 10 mg/100 g BW, i.p.), with supplemental injections (2 mg/100 g BW) given at approximately 90-minute intervals. The trachea was intubated to ensure a patent airway, and the femoral artery and vein were cannulated for measurement of systemic arterial blood pressure and drug injection, respectively. The rectal temperature was maintained at 37° ± 1° C with a heating mat.

The left parietal cortex was exposed by removing virtually the entire parietal bone along its suture line with a dental burr (0.5 mm), which was cooled by air and saline during the surgery. The dura mater was cut such that large vessels were not damaged and minimal bleeding occurred. The brain surface was superfused with a bicarbonate-buffered physiological solution[5] with a Po_2 of 40–45 mm Hg, PCO_2 of 38–43 mm Hg, and pH of 7.35–7.45. The suffusate temperature was maintained at 37° ± 1° C, and the flow rate (3–4 ml/min) was adjusted to minimize atmospheric gas contamination of the fluid. This approach replenished the suffusion solution over the tissue at least three times per minute.

Systemic arterial blood pressure was measured in a femoral artery with a Statham p23Db pressure transducer. Micropressures were measured with a servo-null pressure measurement system (Instrumentation for Physiology and Medicine, Inc., San Diego, California), which was calibrated with a water manometer and which employed sharpened micropipettes with tip diameters less than 1.5 μm. Vessel diameters were measured from videotaped images with a video-splitting device (Indianapolis Center for Advanced Research, Indianapolis, Indiana). A Nikon SKE microscope was used to provide images for an RCA 1020 video camera, and images were videotaped for subsequent playback. Water immersion microscope objectives (× 10, n.a. = 0.22; × 20, n.a. = 0.33) were used to avoid resolution problems caused by the curved air-water interface. A quartz-iodine, 100 watt lamp powered by a precision-regulated DC power supply (Hewlett Packard Model 62012G) was used as a light source. A fiber optic bundle provided illumination of the brain surface at an angle of 25°–35°. The angle of incident illumination greatly enhanced the visual image of the vessel wall whereas angles approaching 90° to the brain surface prevented observation of the vessel wall.

Blood flow velocity was measured in arterioles with internal diameters between 25 and 60 μm, with an on-line velocity tracking correlator (Instrumentation for Physiology and Medicine, San Diego, California). The system was calibrated using epiilluminated glass capillaries (25–70 μm, inner diameter) pump-perfused with whole blood. Details of this calibration procedure have been published recently.[20] Recorded velocity was divided by an empirically determined calibration factor of 1.2 to calculate mean blood flow velocity.[20] Flow was calculated by multiplying the mean velocity by the internal cross-sectional area of the vessel. Flow (in mm^3/sec) was then converted to the percentage of control for presentation in the Results section.

Variations in systemic arterial blood pressure were induced by: 1) hemorrhage into a heparinized syringe to lower pressure; 2) infusion of the shed blood to raise pressure; and 3) intravenous infusion of norepinephrine (25 μg/ml, Sigma Chemical Company, St. Louis, Missouri) to raise arterial pressure. Norepinephrine solutions were buffered to physiological pH and were used on the day prepared. In all cases, the vascular responses to a blood pressure change were allowed to reach a steady-state before data were collected.

Photomicrographs of the cerebral surface at low magnification (× 50) were obtained using a Nikon M-35S film holder and a Nikon PFM photomicrographic adapter. The illumination system remained essentially unchanged, although light intensity was occasionally adjusted to provide maximum contrast. Care was taken to prevent suffusion fluid from welling up over the preparation, since this would result in unpredictable alterations in overall magnification. Using a × 4 objective to provide a large field of view, photographs were taken of the visible brain surface in each animal at rest and during maximum dilation induced by topically applied adenosine (10^{-4} M). Without changing any of the system optics, a photograph was taken of a stage micrometer (0.1 and 0.01 mm, Bausch and Lomb) to provide a measure of distances. The negatives of both the stage micrometer and the cerebral surface were then projected at a set magnification for counting the number of each type of vessel per unit surface area of

brain tissue. The counting procedure was executed blindly, without knowledge of the animal type (WKY or SHR) to which each slide corresponded. The vessel number data, together with the corresponding tissue surface area measurements, were matched with the appropriate animal group, and averages of the number of vessels per square millimeter of brain surface were calculated for each vessel type in WKY and SHR. Data for surface area that corresponded to a given photograph were obtained by tracing the particular area under study on a computer digitizing pad (Apple II Plus computing system). The numbers of vessels seen to open with adenosine application for each animal type were also compared.

In a typical experiment, the animal was allowed to recover for a minimum of 30 minutes after all surgery was completed. Evidence of damage to 5% or more of the tissue, such as petechial hemorrhage or torn cortex, or inability of the 2A and 3A arterioles to dilate at a minimum by 50% when adenosine (10^{-3} M) was topically applied was grounds for termination of the experiment. Data collection was stopped if the control arterial pressure was not spontaneously recovered after a series of pressure changes or after the vessel diameters failed to return to normal.

Each experiment began with the photomicrograph protocol, both in the resting state and after topical adenosine. Following return to steady state, vessels were selected randomly for resting micropressure measurements. This step was followed by a study of autoregulatory responses to changes in blood pressure for randomly selected vessels, during which inner vessel diameter and red cell velocity were simultaneously recorded in first-order arterioles. Micropressures were measured in the largest arterioles and venules during blood pressure manipulations. Initial and subsequent electrode penetrations were sufficiently downstream (100–500 μm) from the point of observation that the pipette did not disturb the section of vessel under study.

Cerebral microvessels were grouped by hierarchical branching pattern as shown in Figure 1. First-order arterioles (1A) were defined as the largest arterioles entering the operative field from beneath the skull and

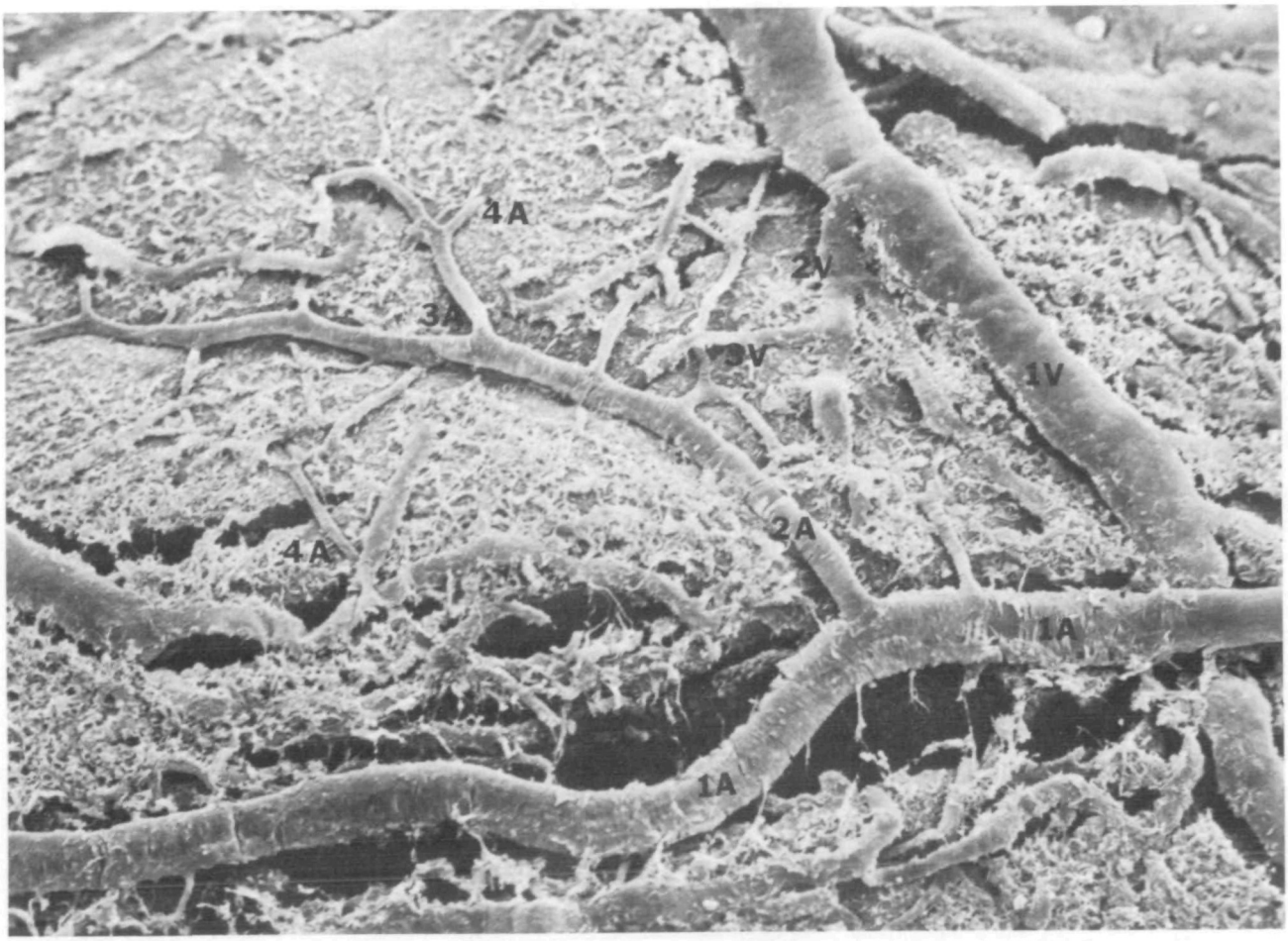

FIGURE 1. *Scanning electron photograph of the rat cerebral cortical vasculature with all vessel types labeled. The spatial arrangement of the vessels as seen in the photograph is identical to the in vivo appearance. Note that arterioles 4A, which are the small vessel branches extending from the 3A, descend into the cortex and are not simply broken (× 100). (Reproduced with the permission of Dr. Andrew P. Evan, Department of Anatomy, Indiana University School of Medicine, Indianapolis, Indiana.)*

are the major branches from the middle cerebral artery. These vessels are representative of the largest arterioles on the brain surface except for a few short vessel segments near the lateral base of the cortex which are part of the middle cerebral artery. Second-order (2A) arterioles branched at nearly right angles from 1A. Likewise, third-order (3A) vessels branched similarly from the 2A. The fourth-order (4A) arterioles branched from 3A and either directly perfused surface capillaries or descended into the cortical parenchyma. That the cortical blood flow to superficial and deep vascular beds is separated has been verified by observing that occlusion of 3A does not result in retrograde flow in 4A. Therefore, measurements of flow in surface vessels represent vascular behavior of the superficial cortical circulation.

Results are presented as means and standard deviation or standard error of the mean, as indicated. Multiple comparison of means was executed using Duncan's new multiple range test[21] at a protection level of 0.05 in the evaluation of significant differences between WKY and SHR. Where appropriate, pairs of means or pairs of slopes were compared using a two-sample t test at the 5% significance level. Multiple linear regression analyses were executed with a computer program based on Sokal and Rohlf.[22]

Results

Lowering arterial pressure by hemorrhage and raising arterial pressure by norepinephrine both will change circulating norepinephrine concentrations and possibly influence cerebral vascular behavior. Direct suffusion of norepinephrine at a concentration equal to that used for intravenous infusion (25 μg/ml) had no effect on the resting diameters of arterioles and venules of WKY and SHR. In a previous study[19] of cerebral autoregulation in the Wistar rat, we developed a protocol to test the effect of intravenously infused norepinephrine when the arterial pressure is held constant. In brief, the vessel diameter at the resting arterial pressure is measured and then norepinephrine is infused until at least a 25 mm Hg increase in pressure occurs. While the infusion continues, the mean pressure is restored to the resting pressure by hemorrhage. The vessel diameters at rest and during the combined norepinephrine infusion with hemorrhage are equal in WKY or SHR. Therefore, intravascular norepinephrine has minor, if any, effects on cerebral microvessels so long as the arterial pressure is held normal for a given strain of rat.

Figure 2 shows the percentage of control blood flow measured in 1A as a function of: 1) the mean arterial pressure; and 2) the percentage of control blood pressure for both WKY (106 vessels in 19 animals) and SHR (119 vessels in 21 animals). Each point represents the average (± SEM) of the steady-state percentage of control flow determinations in a 10 mm Hg range of blood pressure, or a 10% of control blood pressure interval, where 100% of control mean arterial blood pressure for the data in this figure equals 122 ± 8 (SD) mm Hg in WKY and 173 ± 14 (SD) mm Hg in SHR. In WKY, the blood flow remained essentially constant over a mean arterial pressure range of 70 to 150 mm Hg. Significant ($p < 0.05$) decreases and increases in the percentage of control flow in WKY occurred at 60 and 160 mm Hg, respectively. In SHR, the percentage of control flow remained constant over the pressure interval 100 to 200 mm Hg. Significant ($p < 0.05$) decreases and increases in the percentage of control flow in SHR occurred at 90 and 210 mm Hg, respectively. The lower and upper limits for maintenance of constant cerebral blood flow in SHR were therefore shifted by increments of +30 mm Hg and +50 mm Hg, respectively.

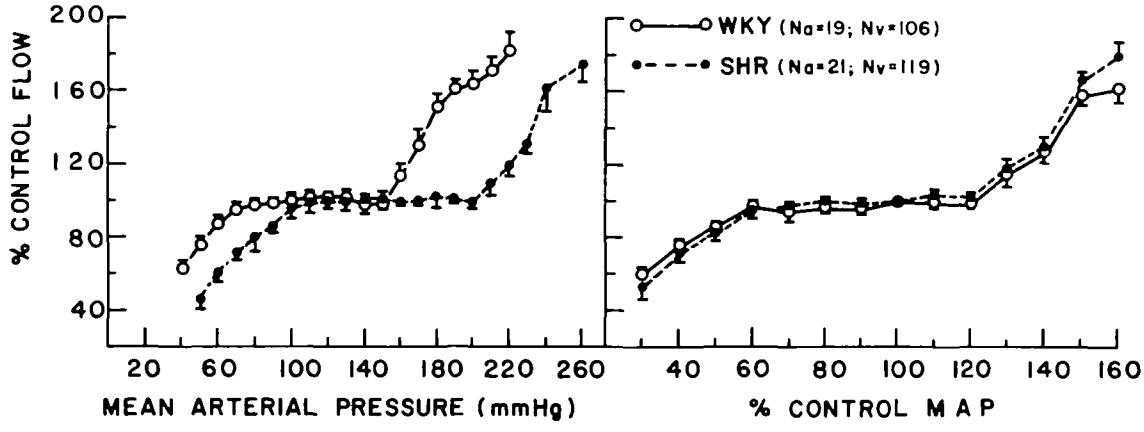

FIGURE 2. *Left: Percentage of control cerebral blood flow as a function of mean arterial pressure. Each point represents the mean ± SEM in a 10 mm Hg pressure interval. Right: Percentage of control blood flow as a function of the percentage of control mean arterial pressure. Each point represents the mean ± SEM in a 10% pressure interval. (Na = number of animals; Nv = number of vessels studied).*

The second portion of Figure 1 depicts the percentage of control blood flow as a function of the percentage of control blood pressure. This format removed the differences in resting systemic pressure from analysis and allowed us to compare blood flow autoregulation for comparable proportional changes in systemic arterial pressure. WKY and SHR demonstrated no difference in the percentage of control blood flow over a systemic arterial pressure range of 50% to 120% of control. In both WKY and SHR, flow was seen to decrease significantly ($p < 0.05$) at 50% of control and increase significantly ($p < 0.05$) at 130% of control blood pressure.

Maximum flow during vessel dilation with adenosine was measured in nine SHR and eight WKY, at the respective resting mean arterial pressures for each species. Expressed as the percentage of control flow, the values for maximum flow were 216.2% ± 15.0% (SE) and 201.1% ± 12.1% for SHR and WKY, respectively, and were not significantly different ($p > 0.2$, two-sample test).

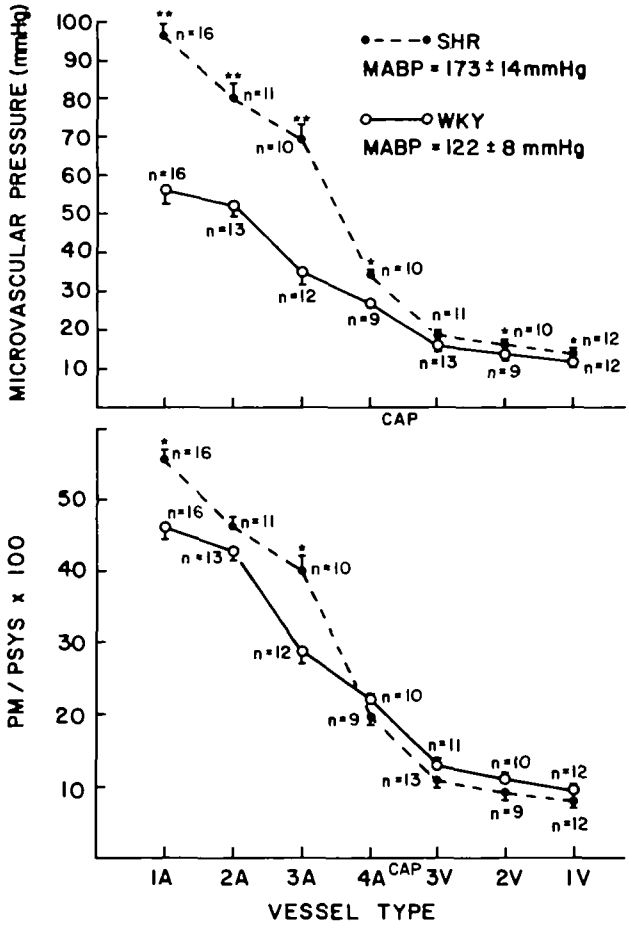

FIGURE 3. *Upper: Microvascular pressure as a function of vessel type. Lower: Normalized microvascular pressure (microvascular pressure divided by systemic pressure) as a function of vessel type. Errors are SEM, and each point equals the mean microvascular pressure or ratio, where n = number of animals. MABP reported is mean ± SD (*p < 0.05; **p < 0.01, WKY≠SHR).*

The resting cortical microvascular pressure distributions for WKY and SHR are illustrated in Figure 3. Each point represents the average (± SEM) of determinations in a particular vessel type for the number of animals shown at each point. Significant differences in pressure ($p < 0.05$) existed between all comparable arterioles in WKY and SHR. Average values for 3V, or smallest venule, micropressure were not significantly different in WKY (15.8 ± 1.2 (SE) mm Hg) and SHR (18.7 ± 1.5 mm Hg). Micropressures in intermediate-sized venules, or 2V, were significantly ($p < 0.05$) higher in SHR (16.3 ± 0.5 mm Hg) compared to WKY (13.8 ± 1.0 mm Hg). Likewise, pressures in the largest venules, 1V, were increased in SHR (14.4 ± 0.6 mm Hg) relative to WKY (12.2 ± 1.0 mm Hg).

Surface capillary pressure measurements were extremely difficult to obtain due to the movement of the brain caused by respiration and the arterial pulse pressure. Consequently, cerebral cortical capillary pressure was assumed to fall within the limits stipulated by the 4A and 3V, the smallest visible arterioles that perfuse capillaries and the venules that drain capillaries, respectively. The lower portion of Figure 2 expresses the microvascular pressure as a fraction of the systemic arterial pressure. Each value is equivalent to the percentage of systemic arterial pressure that remained at the point of measurement in a particular vessel type. The ratio of microvascular to systemic arterial pressure was elevated significantly ($p < 0.05$) in the SHR 1A compared to WKY 1A. This indicated that a proportionately greater fraction of the systemic arterial pressure was transmitted through the cerebral arteries to the microvasculature in SHR (55.5%) compared to WKY (46%). In effect, the large arterial vessels preceding the 1A in WKY dissipated a larger fraction of the arterial pressure than did similar vessels in SHR. The microvascular to systemic pressure (Psys) ratio was not significantly different at the level of the 2A, which indicated that equivalent fractions of the arterial pressure were dissipated by the 1A and branch section to 2A in both animal types. The 3A/Psys ratio was significantly ($p < 0.05$) increased in SHR, but became statistically equal to that of the WKY in all vessels from the 4A (smallest arterioles) to the 1V (largest venules), inclusive. The greatest pressure drop in the microvasculature occurred between the 2A and 3A (approximately 17 mm Hg) in WKY, and between the 3A and 4A in SHR (approximately 34 mm Hg).

Figure 4 shows the percentage of control resistance as a function of the percentage of control arterial pressure for both the microcirculation (RMC) and the arterial vessels upstream from the microcirculation (RLA), in both WKY and SHR. Each point represents the mean (± SEM) of resistance calculations in a 10% pressure interval in 11 WKY and nine SHR. RMC was calculated as shown in Equation 1. The resistance cal-

culated was a relative index, since the percentage of control flow rather than flow per mass tissue was used:

$$RMC = P1A - P1V/\%\ \text{control flow} \quad (1)$$

where P1A and P1V are pressures in 1A arterioles and 1V venules, respectively, at each 10% interval of systemic arterial blood pressure. RLA was calculated as

$$RLA = Psys - P1A/\%\ \text{control flow} \quad (2)$$

where Psys and P1A are systemic arterial and 1A arteriolar blood pressures at each 10% increment of systemic arterial pressure. The percentage of control flow terms in Equations 1 and 2 is equal for a given 1A pressure. The percentage of control flow in the microvasculature and arteries that precedes the microvasculature must be equal, because these vascular segments are in series. There is a possibility that this condition can be disrupted if the number of microvessels in which flow occurred is altered as Psys is changed. However, we found no evidence of the opening of previously closed vessels, or vice versa, in 1A, 2A, 3A, and 4A as the arterial pressure was changed. This indicated that the number of microvessels opened to flow was not altered as the arterial pressure was changed. Thus, we can assume that the relative flow changes in microvessels and upstream large arteries are equal.

At arterial pressures from 40% to 160% of control in both WKY and SHR (100% control pressure = 119 ± 9 (SD) mm Hg in WKY and 168 ± 10 (SD) mm Hg in SHR), RMC changed by proportionately identical amounts, as demonstrated by the superimposition of the curves (Figure 3). Both WKY and SHR demonstrated equivalent increases in RMC up to 120% of the control mean arterial pressure, followed by a comparable fall in RMC per additional incremental increase in the percentage of control blood pressure above 120% of control.

Although there were occasionally significant differences ($p < 0.05$) between large artery relative resistances (RLA) within a given pressure interval, there appeared to be no substantial difference over the entire pressure range studied for WKY and SHR (Figure 4). As seen in Figure 4, there may be an overall increase in the percentage of control RLA for SHR above 110% of control arterial pressure, even though the curves for both WKY and SHR have qualitatively similar slopes at high pressures. Regardless of animal type, RMC decreased proportionately more ($p < 0.05$) than RLA at pressures below 70% of control.

Linear regression analysis of the percentage of control resistance vs the mean arterial pressure (mm Hg) was executed for both RLA and RMC in each animal type for arterial pressures below 120% of the control pressure. This was done to provide a measure of actual change in relative resistance per incremental change in mean arterial pressure (mm Hg). In the equations below, Y = % of control resistance and X = mean arterial pressure in mm Hg:

For RLA (errors are SEM), WKY: $Y = 0.62\ (\pm 0.03)\ X + 25.35\ (\pm 3.26)$; $r = 0.991$; SHR: $Y = 0.42\ (\pm 0.05)\ X + 32.92\ (\pm 5.41)$; $r = 0.951$. The SHR slope is significantly less than the WKY slope ($p < 0.02$).

For RMC (+ SEM), WKY: $Y = 0.81\ (\pm 0.03)\ X + 1.51\ (\pm 0.62)$; $r = 0.996$); SHR: $Y = 0.52\ (\pm 0.03) + 10.38\ (\pm 2.49)$; $r = 0.987$). The SHR slope is significantly less than the WKY slope ($p < 0.001$).

These results indicate that there is a smaller percentage of change in resistance in the SHR for equivalent changes in mean arterial pressure (mm Hg) relative to

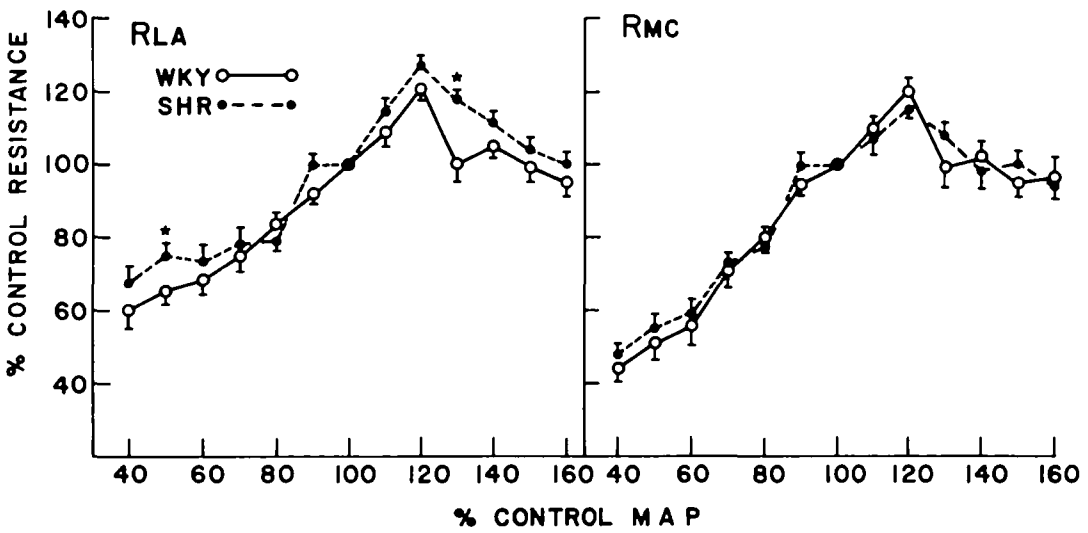

FIGURE 4. *Percentage of control resistance (RLA or RMC) as a function of the percentage of control mean arterial pressure. Each point represents the mean calculated relative resistance (errors are SEM) in 11 WKY and nine SHR. 100% of control mean arterial pressure = 119 ± 9 (SD) mm Hg in WKY and 168 ± 10 mm Hg in SHR;* *$p < 0.05$, *WKY≠SHR.*

TABLE 1. *Arteriolar Dimensions in 18 to 21-Week-Old WKY and SHR*

Vessel type	Resting diameter (μ)	Passive diameter (μ)	Wall thickness (μ)	Wall thickness (diameter)	Wall area (μ^2)
1A-WKY (19)	51.2±3.3	71.2±4.3	6.02±0.64	0 13±0.01	1126±102
1A-SHR (21)	42.5±2.1*	66.5±5.8	7.74±0.94*	0.18±0.02*	1325±90*
2A-WKY (19)	34.3±2.2	47.0±3.5	5.69±0.31	0.18±0.02	624±44
2A-SHR (21)	27.1±2.0*	45.2±3.1	5.81±0.53	0.22±0.02*	714±77
3A-WKY (19)	21.6±1.3	35.3±1.6	4.08±0 42	0.19±0.01	328±26
3A-SHR (21)	21.1±1.0	34.5±1.1	4.43±0.26	0.21±0.02	355±30
4A-WKY (19)	12.5±0.6	18.2±1.4	3.80±0.10	0.32±0.03	194±16
4A-SHR (21)	9.4±0.4*	16.6±0.8	4.32±0.29*	0.46±0.05*	255±20*

All values are means ± 1 SEM. The number of animals studied is given in parentheses.
*$p < 0.05$, WKY vs SHR.

the WKY. As previously mentioned, if relative resistance changes are compared on the basis of the percentage of control arterial pressure, the relationships are essentially identical in WKY and SHR.

Table 1 presents data for both vessel wall parameters and microvascular pressure parameters in WKY and SHR in their respective resting states. The vessel wall characteristics shown are from 122 vessels in 19 WKY, and 140 vessels in 21 SHR. Significant ($p < 0.05$) constriction of 1A, 2A, and 4A occurred at rest in SHR compared to WKY, although passive diameters were not different ($p > 0.05$) for any vessel type so long as the animals were at their respective natural resting arterial pressures. There was a significant ($p < 0.05$) increase in vessel wall thickness for 1A and 4A in SHR, as well as an increase in wall thickness/lumen diameter ratio for 1A, 2A, and 4A. In 1A and 4A, there was a significant ($p < 0.05$) increase in vessel wall cross-sectional area which indicated hypertrophy of these vessels. The increase in the ratio of wall thickness/lumen diameter for 1A and 4A resulted from a combination of both the decrease in resting diameter and hypertrophy of the vessel wall. Resting diameters (mean ± SEM) for venules were as follows: 3V (smallest venules), WKY = 31.6 ± 4.1 μm, SHR = 34.2 ± 5.0 μm; 2V (intermediate), WKY = 76.2 ± 8.1 μm, SHR = 81.9 ± 6.8 μm; 1V (largest), WKY = 160.6 ± 10.7 μm, SHR = 164.5 ± 10.9 μm. These data indicate that the diameters of comparable types of venules in WKY and SHR are not different ($p > 0.05$) at rest.

Table 2 shows major and significant ($p < 0.01$) increases in resting microvascular pressures in the 1A, 2A, and 3A of SHR, with a small but significant ($p < 0.05$) increase in pressure evident in the 4A. In spite of the increases in microvascular pressure, a significant increase in resting wall stress (calculated as the product of resting microvascular pressure and vessel radius divided by vessel wall thickness) was found only in the 3A, with statistically equal ($p > 0.05$) wall stresses in 1A, 2A, and 4A of WKY and SHR.

The vascular density characteristics (Table 3) showed no differences ($p > 0.05$) in vascular density expressed as the number of vessels per square millimeter of cerebral surface tissue for 1A, 2A, or 3A in SHR and WKY. In addition, there was no difference in either WKY or SHR in the number of vessels (1A, 2A, or 3A) counted before and after passive conditions were initiated. These data for resting and passive conditions indicated that there was no significant element

TABLE 2 *Arteriolar Wall Stress in 18- to 21-Week-Old WKY and SHR*

Vessel type	No.	Microvascular pressure (mm Hg)	Resting wall stress ($\times 10^4$ dyn/cm^2)
1A-WKY	16	55 6±5.0	29.8±2.4
1A-SHR	16	96.0±4.4†	35.5±4.4
2A-WKY	13	51.8±3.3	19.8±3.2
2A-SHR	11	79.8±4.0†	24.0±4.7
3A-WKY	12	34.6±3.1	11.9±0.6
3A-SHR	10	68.9±4.9†	19.7±2.9†
4A-WKY	9	27.2±1.0	5.1±0.2
4A-SHR	10	34.0±1.6*	5.5±0 3

All values are means ± 1 SEM.
*$p < 0.05$, WKY vs SHR.
†$p < 0.01$, WKY vs SHR.

TABLE 3. *Cerebral Cortical Surface Vascularity Characteristics of 18- to 21-Week-Old WKY and SHR*

Vessel type	WKY (n = 8)	SHR (n = 8)	p
1A/mm^2 tissue	0.30±0.04	0.26±0.04	NS
2A/mm^2 tissue	0.76±0.11	0.67±0.07	NS
3A/mm^2 tissue intact	1.78±0.14	1.61±0.10	NS
3A/mm^2 tissue passive	1.82±0.14	1.64±0.11	NS
Tissue surface area (mm^2)	16.42±0.57	17.28±0.66	NS

Values are means ± 1 SEM.

of temporary or permanent vascular closure in either animal type.

Figure 5 presents the diameter responses of 122 vessels in 19 WKY and 140 vessels in 21 SHR over the arterial pressure range shown. Each point shown reflects the average of the diameter determinations in a 10 mm Hg steady-state pressure interval for a given animal type. Multiple linear regression analysis[22] of the data for vessels produced second-order equations for best-fit lines through each set of points corresponding to a particular vessel and animal type. Resting lumen diameter for arterioles are shown in Table 1. In the 1A, the SHR exhibits smaller diameters than WKY throughout the range of pressures studied. The 2A demonstrated slightly smaller diameters in SHR than in WKY at pressures below about 120 mm Hg. At higher pressures, the 2A in SHR had diameters substantially less than those in WKY. The 3A vessels in both SHR and WKY were similar in diameter at low pressures (<90 mm Hg), although the SHR demonstrated smaller diameters than WKY at higher pressures (>100 mm Hg). In the 4A, roughly similar diameters were found for WKY and SHR in low pressure ranges (<90 mm Hg), but diameters for SHR were substantially less at midrange and high pressures. At arterial pressures above 170 mm Hg, the WKY rat will develop alternating areas of constriction and dilation along the arterioles. The behavior typically subsides when a normal arterial pressure is established; if the behavior did not cease, the experiment was stopped. The SHR did not display this behavior even at arterial pressures of 250 mm Hg.

Figure 6 depicts the same data and relationships as in Figure 5, except that the diameters and pressure intervals are expressed as the percentage of control values for each animal and vessel type. This type of relationship allows one to compare relative diameter changes in normal and hypertensive animals for proportionately equal changes in arterial pressure. Thus, 100% of control mean arterial pressure equals 122 ± 8 (SD) mm Hg in WKY and 173 ± 14 (SD) mm Hg in SHR for these data. Below 90% of control mean arterial pressure, the percentage of increase in 1A diameter was greater in WKY than SHR. Approximately equal percentage changes in the diameter of 1A in WKY and SHR occur at pressures above 90% of control. For 2A, 3A, and 4A, SHR and WKY showed similar percentage changes in diameter for equivalent percentage changes in mean arterial pressure throughout the pressure range studied.

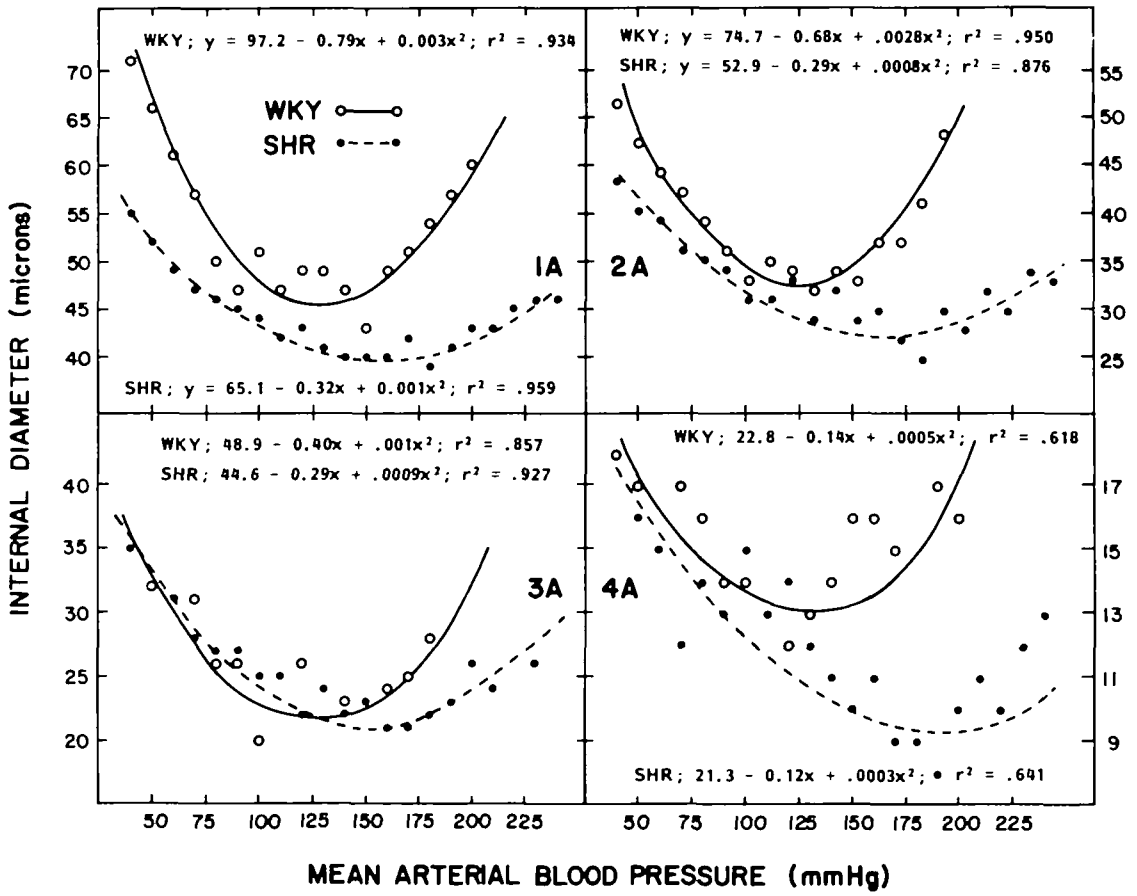

FIGURE 5. *Vessel diameter as a function of mean arterial blood pressure in 19 WKY and 21 SHR. Each point represents the mean of all observations for a particular vessel type in a 10 mm Hg pressure interval. Equations are for best-fit lines through the points shown.*

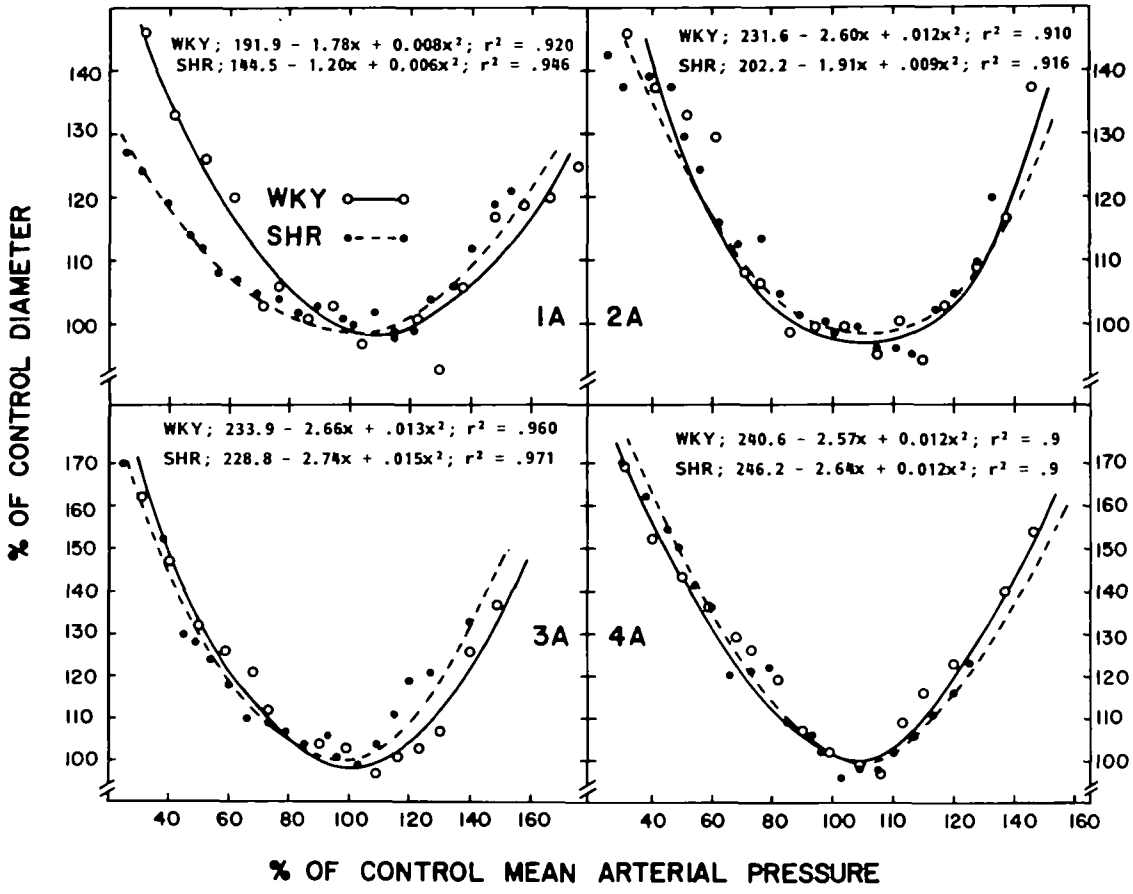

FIGURE 6. *Percentage of the control vessel diameter as a function of the percentage of control mean arterial pressure. Each point represents the mean of all observations for a particular vessel type in a 10% of control pressure interval. Equations are for best-fit lines through the points shown.*

Discussion

The results of this study indicate a resetting of the cerebral blood flow (CBF) autoregulatory range to substantially higher systemic arterial pressures in the adult SHR (Figure 2). Even though arteriolar pressures were elevated (Figure 3), the small venule and, presumably, capillary pressures were near normal despite systemic hypertension. As will be subsequently discussed in detail, arteriolar constriction and related vessel wall hypertrophy were the primary physical means to both reset the autoregulatory pressure range and protect microvascular pressures in the exchange vasculature.

The mechanisms for increasing the vascular resistance in SHR are generally considered to include: 1) arteriolar constriction; 2) arteriolar wall hypertrophy, which augments constriction; and 3) microvascular rarefaction, or diminished numbers of arterioles open to flow. There is substantial heterogeneity in the relative importance of the aforementioned mechanisms for flow and resistance regulation in a variety of tissues, which suggests that a universal format for microvascular adaptation to hypertension may not exist.

In the present study, we noted (Table 1) that the 1A (largest), 2A, and 4A (smallest) arterioles in the cerebral cortex of SHR were significantly constricted compared to similar vessels of WKY. Since microvascular rarefaction was absent (Table 3), constriction was the major cause of increased resistance in the cerebral vasculature. These observations of vessel constriction in the SHR brain are similar to those by Bohlen[23] in the small intestine of SHR, which also demonstrated constriction of largest and smallest arterioles and minimal rarefaction. However, no vasoconstriction compared to WKY was seen in studies of cremasteric,[11-14] gracilis,[15] or spinotrapezius[16] muscle vasculatures in SHR. Thus, the vasculatures of the brain and intestine in the adult SHR follow a very similar format of generalized vasoconstriction to increase vascular resistance, although neither vascular bed manifests the substantial rarefaction found in the skeletal muscle vasculatures.

Folkow et al.[24] proposed that vascular wall hypertrophy and an associated increase in the wall thickness/lumen diameter ratio were major elements in the course of sustained hypertension. Hart et al.[10] have demonstrated substantial hypertrophy in cerebral pa-

renchymal arterioles (<35 μm, internal diameter) of the stroke-prone SHR. The present study corroborates the findings of Hart et al.[10] that cerebral vessels undergo hypertrophy, with two important differences: 1) we studied the stroke-resistant SHR rather than the stroke-prone strain; and 2) our results reflect in vivo measurements, while Hart et al.[10] used a perfusion-fixation technique with subsequent histological analysis. Although our present study does not address the cause of vasoconstriction, it may be partially based on the presence of vascular wall hypertrophy. The hypertrophy of 1A and 4A (Table 1) caused the ratio of wall thickness/lumen diameter to increase such that wall stress was normal in spite of increased microvascular pressure. The 2A did not experience wall hypertrophy, but vasoconstriction caused an increase in wall thickness/lumen diameter ratio such that wall stress in the 2A of SHR was statistically equal to that found in WKY. The resting wall stress in the 3A of SHR was significantly elevated above that in WKY (Table 2). However, there was an average 66% increase in wall stress of the 3A in SHR, compared to an average 100% increase in 3A intravascular pressure. The fact that wall stress increased less, relative to the increase in microvascular pressure, indicates that the slight wall hypertrophy and constriction of 3A helped to maintain a normal wall stress, just as in the 1A, 2A, and 4A of SHR.

The elevation of microvascular pressures in the arterioles of the SHR, as shown in Figure 2, would be a stimulus for vessel wall hypertrophy, if this hypothesis[24] is correct. The vessel wall hypertrophy and vasoconstriction may be important elements in the protection of cerebral exchange vessels against disruption of the blood brain barrier, as suggested by Hart et al.[10] and Mueller et al.[25] Apparently, the combined effects of arteriolar constriction and wall hypertrophy allow the cerebral arterioles to operate in a normal wall stress range, such that the vessels are not subject to overdistension and potential damage and capillary pressure is maintained near normal (Figure 3). In normal cats[26] and rats (present study) subjected to acute elevations in arterial pressures, the arterioles develop a "sausage-string" appearance due to alternating areas of constriction and dilation along a segment of vessel. This sausage-string pattern was never seen in the arterioles of SHR in the present study, even when mean arterial pressure was acutely elevated as high as 250 mm Hg. The vessels have therefore adapted to chronic hypertension so that they can withstand grossly elevated microvascular pressures without overt physical evidence of vessel wall damage. The arterioles of SHR apparently adapt to elevated pressures by decreasing passive vessel wall distensibility. Evidence supporting a decreased passive distensibility is shown in Table 1, which demonstrates normal passive (maximum) arteriolar diameters in SHR relative to WKY despite major increases in resting microvascular pressures. If the SHR arterioles did not have less distensible than normal walls during passive conditions (no muscle activity), then one would expect resting passive diameters to be significantly greater in SHR due to the elevated microvascular pressures. One would also expect diameters in SHR at very low arterial pressures to be comparable to those in WKY, when in fact they are smaller (Figure 4). The extent to which increased passive stiffness in SHR is due to wall hypertrophy or connective tissue proliferation is unknown. The cost of this protection from wall overdistention and disruption, however, is a smaller than normal diameter at low systemic arterial pressures, such that CBF cannot be precisely regulated at arterial pressures below 100 mm Hg (Figure 1).

Very little data exist on the autoregulation of CBF in the SHR compared to WKY. Fujishima and Omae[9] estimated an upward shift of 33 mm Hg in the lower limit of CBF autoregulation in SHR, which is similar to the 30–35 mm Hg shift seen in the present study (Figure 2). The results of Barry et al.[3] in SHR and those by Loomis[27] in renal hypertensive rats (RHR) demonstrated a 20 mm Hg shift in the lower limit of CBF autoregulation compared to WKY. Barry et al.[3] suggest that structural adaptation, rather than sympathetic or humoral factors, accounts for this shift, since the same shift was seen in both SHR and RHR. Strandgaard et al.[28] have demonstrated a shift in the upper limit of autoregulation during hypertension in the baboon and have suggested that this shift might be due to preexisting vasoconstriction or sympathetic activity. Our results (Figure 2) show upward shifts of both the lower autoregulatory limit (+30 mm Hg) and the upper limit (+50 mm Hg) due to both active vasoconstriction and decreased distensibility. Our study is the first to quantify the shift in the upper autoregulatory limit for the SHR relative to WKY. Further, our results (Table 1) suggest that this shift is probably related to vascular wall hypertrophy, since such a condition would: 1) raise the lower limit of CBF autoregulation in SHR by preventing normal vessel dilation at low perfusion pressures; and 2) raise the upper limit of autoregulation by potentiating the ability of SHR vessels to constrict at higher perfusion pressures.

Our present study demonstrates that near normal cerebral capillary pressures may exist in the SHR, despite a gross elevation of systemic arterial pressure. The exchange vasculature of the SHR brain is apparently protected from high pressures by upstream vasoconstriction, especially in the smallest precapillary vessels (4A) (Figure 3). Similar circumstances have been found in the intestinal microvasculature by Bohlen[23] and the skeletal muscle vasculature by Zweifach et al.,[16] in spite of the absence of microvascular wall hypertrophy in the latter. Further, these studies[16, 23] suggest that the small arterioles, such as 3A and 4A, are responsible for most of the protective effects seen for capillary pressure. Thus, it appears that the very smallest arterioles have the greatest responsibility in assuring relatively normal capillary pressures. In spite of tissue-related heterogeneity in hypertensive vascular adaptation (i.e., wall hypertrophy and/or rarefaction vs lack thereof) the end result appears to be the same: protection of the exchange vasculature from high pressure and overperfusion.

Microvascular rarefaction, whether due to a permanent loss of arterioles, temporary closure of arterioles, or a combination of these factors, is not evident in the cerebral cortical circulation of the SHR (Table 3). Thus, the increase in vascular resistance in the brain of the SHR must be due primarily to vasoconstriction, as previously discussed. Similar absences of rarefaction of small arterioles have been noted in studies of the intestinal microcirculation[23] and the renal microvasculature.[29] However, rarefaction is present in various skeletal muscle vasculatures during sustained hypertension.[11-15] It is possible that the vascular architecture in different tissues accounts for differences in vessel rarefaction during hypertension. For example, the muscle vasculature is generally arranged such that multiple arterioles can perfuse an area of tissue, although individual capillaries are usually perfused by only one arteriole. By contrast, the brain, kidney, and intestine appear to perfuse an area of tissue with a single arteriole. Consequently, focal absence of temporary closure of a small vessel in the brain, kidney or intestine might result in infarcted or severely ischemic tissue.

The vessels upsteam from the cerebral microcirculation have been demonstrated to make significant contributions to blood flow regulation in the cat[17, 18, 31] and rat.[19] In WKY of the present study, vessels upstream from the microcirculation contributed a significantly greater percentage of total resistance (54%) than did the large vessels in the SHR (45.5%), at resting mean arterial pressures (Figure 3). This suggests that, in order to keep capillary pressures in a normal range, the SHR must manifest a greater portion of its total vascular resistance in the microcirculation. However, the fact that the arterial vasculature of SHR contributed proportionately less to vascular resistance than in WKY does not imply that the large vessels in SHR fail to adapt during hypertension.

As shown in Figure 4, RMC and RLA change by proportionately similar amounts in SHR and WKY. This indicates that the large vessels upstream from the microcirculation in SHR retain their ability to contribute to autoregulation even though the pressures in these vessels are increased by 40% to 45%. It is also interesting to note that, regardless of animal type, RMC tends to decrease more than RLA at low arterial pressures. Thus, the microvessels make a greater contribution to flow regulation at low arterial pressures. Perhaps the most important implication of the data in Figure 4 is that the upward shift in the autoregulatory range that occurs in the SHR relative to WKY appears to involve both the cerebral macro- and microvasculature. Even though structural adaptation of the vessel walls is evident in SHR, the regulatory characteristics of the vasculature are similar to those in WKY. The response patterns of flow (Figure 2), vessel diameter (Figure 6), and relative resistance of large (RLA) and small (RMC) vessels (Figure 4) overlap where differences in mean arterial pressure are normalized. It is as if the normal response pattern of WKY had been preserved in SHR but adapted to a higher range of arterial pressures. For this to occur, the existing control mechanism may experience a decreased gain; that is, the relative resistances of microvessels (RMC) and arteries (RLA) change by smaller amounts in SHR than in WKY for equal changes in arterial pressure, as demonstrated by the regression analysis in the Results section.

Acknowledgments

The authors thank Kim Hankins for technical assistance, and Marsha Hunt for typing the manuscript.

References

1. Byrom FB. The hypertensive vascular crisis. An experimental study. London: W. Heineman Medical Books, Ltd., 1969
2. Byrom FB. The pathogenesis of hypertensive encephalopathy and its relation to the malignant phase of hypertension: experimental evidence from the hypertensive rat. Lancet 1954; 2:201–211
3. Barry DI, Strangaard S, Graham DI, et al. Cerebral blood flow in rats with renal and spontaneous hypertension: resetting of the lower limit of autoregulation. J Cereb Bl Flow Metab 1982;2:347–353
4. Hoffman WE, Miletich DJ, Albrecht RF. Maintenance of cerebral blood flow and metabolism during pharmacological hypotension in aged hypertensive rats. Neurobiol Aging 1982; 3:101–104
5. Yamori Y, Hone R. Development course of hypertension and regional cerebral blood flow in stroke-prone spontaneously hypertensive rats. Stroke 1977;8:456–461
6. Strandgaard S. Autoregulation of cerebral blood flow in hypertensive patients: the modifying influence of prolonged antihypertensive treatment on the tolerance to acute drug-induced hypotension. Circulation 1976;53:720–726
7. Strandgaard S, Oleson J, Skinhoj E, Lassen NA. Autoregulation of brain circulation in severe arterial hypertension. Br Med J 1973;1:507–511
8. Strandgaard S. Autoregulation of cerebral circulation in hypertension. Acta Neurol Scand 1978;57(Suppl 66):1–82
9. Fujishima M, Omae T. Lower limit of autoregulation in normotensive and spontaneously hypertensive rats. Experientia 1976;32:1019–1021
10. Hart MN, Heistad DD, Brody MJ. Effect of chronic hypertension and sympathetic denervation on wall/lumen ratio of cerebral vessels. Hypertension 1980;2:419–423
11. Bohlen HG. Arteriolar closure mediated by hyperresponsiveness to norepinephrine in hypertensive rats. J Appl Physiol 1979;236:H157–H164
12. Chen IIH, Prewitt RL, Dowell RF. Microvascular rarefaction in spontaneously hypertensive rat cremaster muscle. Am J Physiol 1981;241:H306
13. Hutchins PM. Arteriolar rarefaction in hypertension. Bibliotheca Anat 1979;18:166–168
14. Hutchins PM, Darnell AE. Observation of decreased numbers of small arterioles in spontaneously hypertensive rats. Circ Res 1974;34 and 35 (suppl I):I-151–I-165
15. Prewitt RI, Chen IIH, Dowell RF. Development of microvascular rarefaction in the spontaneously hypertensive rat. Am J Physiol 1982;243:H243–H251
16. Zweifach BW, Kovalchek C, DeLano F, Chien P. Micropressure-flow relationships in a skeletal muscle of spontaneously hypertensive rat. Hypertension 1981;3:601–614
17. Kontos HA, Wei EP, Navari RM, Levasseur JE, Rosenblum WI, Patterson JL Jr. Responses of cerebral arteries and arterioles to acute hypotension and hypertension. Am J Physiol 1978;234:H371–H383

18. Stromberg DD, Fox JR. Pressures in the pial arterial microcirculation of the cat during changes in systemic arterial blood pressure. Circ Res 1972;31:229–239
19. Harper SL, Bohlen HG, Rubin MJ. Arterial and microvascular contributions to cerebral cortical autoregulation in rats. Am J Physiol 1984;246:H17–H24
20. Harper SL, Bohlen HG. *In vitro* and *in vivo* measurement of red cell velocity measurement with epi- and transillumination. Microvas Res 1983;25:186–193
21. Steel RGD, Torie JH. Principles and procedures of statistics. New York: McGraw Hill, 1960:107
22. Sokal PR, Rohlf FJ. Linear regression. In: Biometrics, 2nd ed. San Francisco: WH Freeman and Company, 1981:454–457
23. Bohlen HG. Intestinal microvascular adaptation during maturation of spontaneously hypertensive rats. Hypertension 1983; 5:739–745
24. Folkow B, Hallback M, Lundgren Y, Silvertsson R, Weis L. Importance of adaptive changes in vascular design for establishment of primary hypertension studied in man and spontaneously hypertensive rats. Circ Res 1973;32 (Suppl I):I-2–I-13
25. Mueller SM, Ertel PJ, Felten DL, Overhage JM. Sympathetic nerves protect against blood-brain barrier disruption in the spontaneously hypertensive rat. Stroke 1982;13:83–88
26. MacKenzie ET, Strandgaard S, Graham DI, Jones JV, Harper AM, Farrar JK. Effects of acutely induced hypertension in cats on pial arteriolar caliber, local cerebral blood flow, and the blood brain barrier. Circ Res 1976;39:33–41
27. Loomis P. Hypertension and necrotizing arteritis in the rat following renal infarction. Arch Pathol 1946;41:231–238
28. Strandgaard S, MacKenzie ET, Sengupta D, Rowan JO, Lassen NA, Harper AM. Upper limit of autoregulation of cerebral blood flow in the baboon. Circ Res 1974;34:435–440
29. Azar S, Tobian L, Johnson MS. Glomerular, efferent arteriole, and peritubular capillary and tubular pressures in hypertension. Am J Physiol 1974;227:1045–1050
30. Judy WV, Watanabe AM, Henry DP, Besch HR, Murphy WR, Hockel GM. Sympathetic nerve activity: role in regulation of blood pressure in the spontaneously hypertensive rat. Circ Res 1976;38(Suppl II):I-121–I-129
31. Baumbach GL, Heistad DD. Cerebral microvascular pressure during sympathetic stimulation (abstr). Fed Proc 1982;41: 1610

Microvascular adaptation in the cerebral cortex of adult spontaneously hypertensive rats.

S L Harper and H G Bohlen

Hypertension. 1984;6:408-419
doi: 10.1161/01.HYP.6.3.408
Hypertension is published by the American Heart Association, 7272 Greenville Avenue, Dallas, TX 75231

Print ISSN: 0194-911X. Online ISSN: 1524-4563